J. Mod. Transport. (2014) 22(4):256–260
DOI 10.1007/s40534-014-0042-2

www.springer.com/40534

MD simulation on the interactions between CH_2 groups and the (001) surface of tungsten

Xianfu Feng · Shuping Tian · Xinkui He · Fujun Gou · Shuiquan Deng · Yong Zhao

Received: 3 December 2013 / Revised: 9 February 2014 / Accepted: 10 March 2014 / Published online: 4 April 2014

Abstract This work studies the angle dependence of the interactions between impinging CH_2 particles of 150 eV with the tungsten surface. The simulations show that the carbon atoms are much more easily bonded to the tungsten atoms than hydrogen atoms, though a few of the latter can also penetrate into the tungsten material. When the incidence angle is greater than 75°, the incident CH_2 particles are reflected without break-ups. Below this angle, a W–C layer of about 0.5 nm is formed with another C, H-rich layer depositing on top of it. The molecular dynamics (MD) approach has proved to be a powerful tool to solve the structural problems at atomic length scale of various materials. Some of its possible applications to the railway track materials have also been discussed.

Keywords Molecular dynamics · First-wall material · Tungsten · Plasma-material interaction

1 Introduction

The plasma-facing components (PFCs) are designed to work in an extreme environment exposing to high energy particles and heat flux from the plasma [1]. However, as the designed extreme conditions in the reaction chamber of ITER (International Thermonuclear Experimental Reactor) are still difficult to realize, theoretical simulations become crucial at this stage [2]. Tungsten steel, a composite material containing C and other transition metals, is now widely accepted as one candidate for the first-wall material because of its high melting point, low sputtering rate, good mechanical properties, resistance to radiation, etc. [2, 3]. The performance of plasma-facing surface under intense transient thermal loads is another critical issue, since the formation of a melt layer may favor the generation of highly activated dust particles [1, 4]. Graphite has been selected as one material in the middle and the lower part of the vertical target of the divertor and as the collection panel in the thermonuclear fusion reactor, for their good outgassing property, low Z character and capability of handling high heat fluxes [2, 5]. However, graphite is prone to physical and chemical sputter due to the low sputtering energy threshold [6], which results in many dust particulates. The formation mechanisms, existing forms and their consequences of various kinds of dust particulates resulting from the plasma first-wall interactions have been systematically studied by many authors [7–11]. Among these dust particulates, hydrocarbon radicals have also attracted intensive studies [7–11]. These works shows that carbon atoms can easily combine with hydrogen or its isotope atoms in the plasma chamber leading to the formation of hydrocarbon groups H_xC_y, which reduces dramatically the performance of the first-wall materials [7–9, 11, 12]. Ohya et al. [13, 14] have investigated the interactions of hydrocarbons with the surfaces of the possible first-wall materials (W, C, W–C), as well as their reflections, dissociations and the redepositions by using Monte Carlo (MC) method, and molecular dynamics (MD) method. Because of the torus-like shape of the plasma chamber, the confined high-energy particles are expected to fly in directions shear to the surface of the first wall. This work, thus focuses on the incident angle dependence of the interactions between CH_2

X. Feng · X. He · S. Deng (✉) · Y. Zhao
Superconductivity and New Energy R & D Center, Southwest Jiaotong University, Chengdu 610031, China
e-mail: s.deng@swjtu.edu.cn

S. Tian · F. Gou
Institute of Nuclear Science and Technology, Sichuan University, Chengdu 610064, China

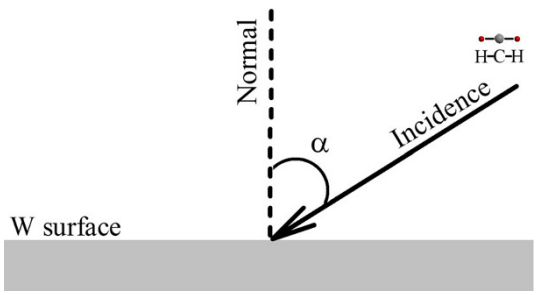

Fig. 1 A scheme of incident angle of CH_2 particles

groups and tungsten surface using MD simulation method. In addition, we have used higher energy flux than the earlier work [13] to investigate the effects of incident energy of such radicals.

2 Computational details

In our MD calculations, all particles in the system are assumed to abide by Newtonian mechanics. The velocity-Verlet method [15] was used for the integration of Newton's equations of motion.

The force on each atom was calculated from the analytical derivative of the modified Tersoff–Brenner potential [16]. This potential consists of the attractive and repulsive terms as shown in Eqs. (1) and (2), respectively.

$$V^{\mathrm{A}}(r) = \frac{SD_0}{S-1}\exp\left[-\beta\sqrt{2/S}(r-r_0)\right], \quad (1)$$

$$V^{\mathrm{R}}(r) = \frac{D_0}{S-1}\exp\left[-\beta\sqrt{2S}(r-r_0)\right], \quad (2)$$

where D_0, r_0, S indicates the dimer bond energy, the dimer bond distance and the adjustable parameter, respectively. The parameter β in Eqs. (1), (2) can be derived from the ground-state oscillation frequency of the dimer. This potential function has been designed specifically for treating the W–C-H system in non-equilibrium state and has been tested in many cases [4, 13, 14, 17].

An $8 \times 8 \times 10$ supercell of the $\alpha - W$ (body-centered cubic) has been chosen as the initial configuration. This model contains 1,280 W atoms, which has a depth of about 3.165 nm and a top surface area of about 6.412 nm^2. The

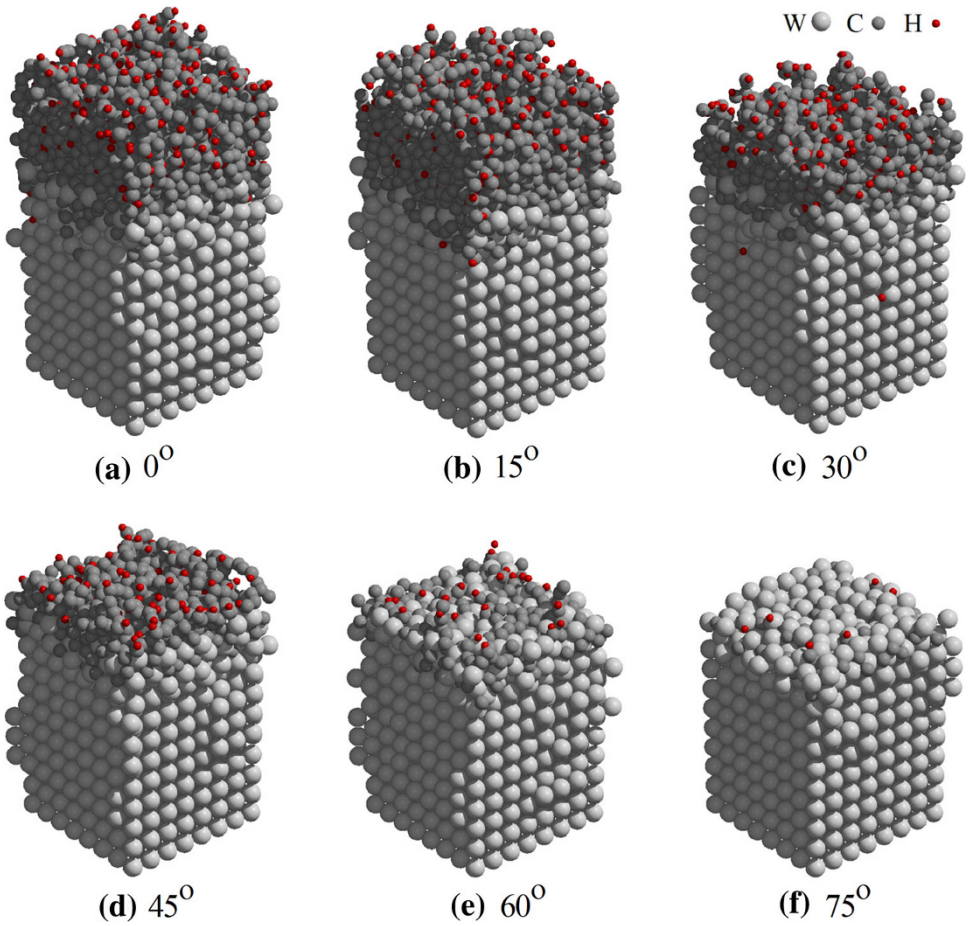

Fig. 2 *Snapshots* of the three simulated surfaces at an incident fluence of 4.09×10^{16} cm^{-2}

(001) plane of $\alpha - W$ is the top surface, i.e., the plasma-facing surface. Periodic boundary conditions are assumed in the a, b directions of the supercell in solving the equations of motion. The bottom layers with a thickness of two-unit cell length are fixed in the simulations. In the simulation, the coupling time between the incident particles and the sample is set to be 0.5 ps with a time step of 0.0005 ps. The initial sample temperature is set to be 300 K. In order to maintain a thermal equilibrium of the system, the BERENDSEN's heat bath technique was used with a BenerdsenTau of 0.01 ps [18]. In this work, the linear H–C–H configuration of CH_2 groups is assumed with the bond axes randomly distributed with respect to the incident direction. In all the cases, the incident energy of CH_2 particles is set to be 150 eV. The incident angle as defined in Fig. 1 is as 0°, 5°, 15°, 30°, 45°, 60°, 75°, and 85°, respectively. The incident fluence is chosen to be 4.09×10^{16} cm^{-2}, a value comparable to those used in other similar simulation works [13, 14].

3 Results and discussion

In Fig. 2, we show snapshots of the bombarded surface of the sample at the chosen incident fluence with three different incident angles. As shown in Fig. 2, both C atoms and H atoms can penetrate into the tungsten surface resulting in a new layer composed of W, C, and H atoms. Our simulations indicate that when the incident angle is less than 45°, a thin "hydrocarbon" layer consisting of mainly C and H atoms is formed on top of the W–C–H layer. When the incident angle is greater than 45°, only W–C–H layer is formed without the upper covering "hydrocarbon" layer.

Figure 3 shows the distributions of the various densities of bonds with respect to the depth in reference to the initial surface. As shown in Fig. 3, the original W surface is smeared with the occurrence of W–W bond distribution above the initial surface. The density of the W–C bonds shows peaks in all of the three cases above the initial surface, which drops rapidly below the initial surface. When the incident angle is less than 30°, the formation of C–C and C–H bonds becomes significant, which indicates the breaking of the incident CH_2 groups (see also Fig. 5). In all the cases, the H–H and W–H bonds are negligible in comparison with the other bonds. It is obvious that the bombardment process results in the displacement of W atoms (see Figs. 2, 3) and the formation of W–C bonding (see Fig. 3) etc.

Figure 4 shows the relations between the numbers of deposited H (a), C (b) atoms and the number of respective incident particulates at different incident angles. As shown in Fig. 4, when the incident angle is smaller than or equal

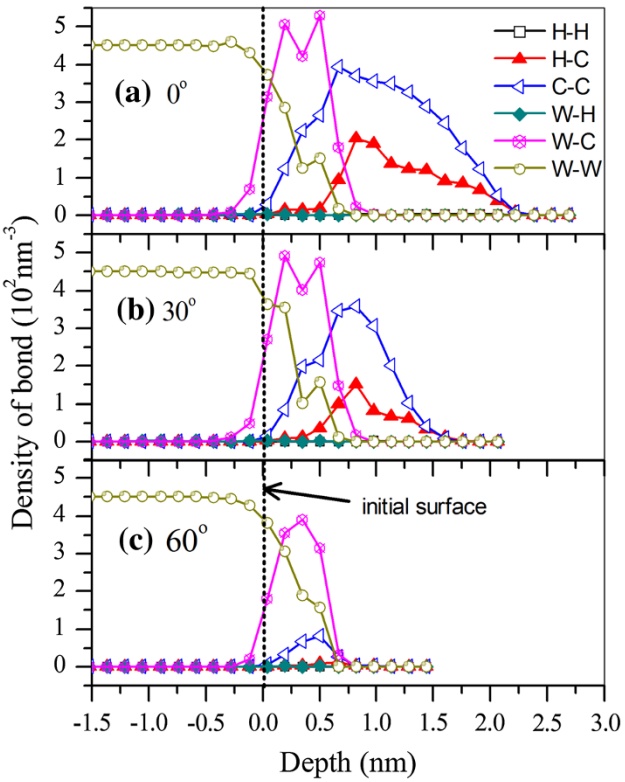

Fig. 3 The bond density distribution along the vertical direction with respect to the initial W (001) surface

to 30° for H and 45° for C, respectively, the deposition is more effective. For both C and H atoms, when the incident angle is larger than 45° for H, 75° for C the deposition rate becomes negligibly small regardless of the density of the incident particles. These results indicate that when the incident direction leans toward the tangent of the surface of the W matrix, the kinetic energy of the incident particles exceeds their bound energy, which invalidates any trapping of the incident particles, and thus the reflection dominates. Figures 3 and 4 clearly show that C atoms are much more easily trapped by the W matrix indicating a stronger bonding between W and C atoms than that between W and H atoms.

Figure 5 shows the incident angle dependence of the relative scattering ratio (RSR) of some important particles produced in the interaction process and the remained CH_2 groups. For clearance, the logarithmic ordinate is used for the RSRs of the indicated particles. As can be seen from Fig. 5, the RSR of C atoms is the lowest in a wide range of incident angles among the scattered particles. Furthermore it has very weak incident angle dependence. In contrast, the RSR of H atoms is the largest among the investigated particles, except for CH_2 radicals whose RSR surpasses all those of the other particles when the incident angle exceeds $\sim$35°, which indicates the dominance of reflection in this range. Considering the following relevant process in the

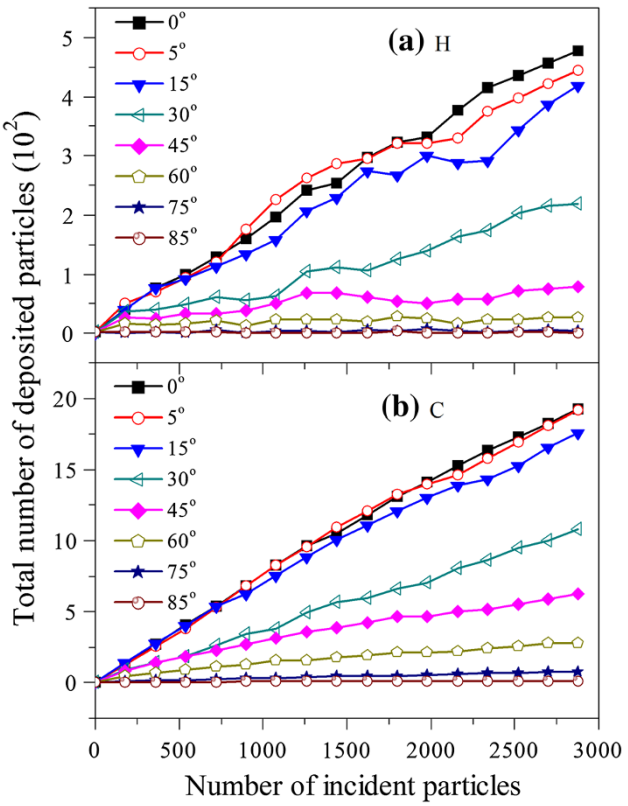

Fig. 4 The relations between the numbers of deposited H (**a**), C (**b**) atoms and the *number* of the respective incident particulates at different incident angles

interactions between the incident CH_2 groups and the W surface,

$$CH_2 \rightarrow H + CH,$$
$$CH_2 \rightarrow 2H + C,$$
$$CH \rightarrow C + H.$$

One can expect that the RSR of C atoms should be approximately two times smaller than that of H atoms, if the above three processes have the similar probability and the relevant particulates are scattered out in the same efficiency. As can be seen from Fig. 5, the RSR of H atoms far exceeds that of C atoms by approximately one order. This may also be possible if the first process dominates, however, considering the results as shown in Figs. 3 and 4, it can be neglected. Taking into account the results shown in Fig. 3, we attribute the origin to be the stronger W–C bonding than the W–H boning. It should be pointed out that the dramatic drop of the scattering ratios for H, C, and CH particles at high incident angles (>75°) results from the reflectance of CH_2 particles, which reduces the source of all C, H, and CH particles.

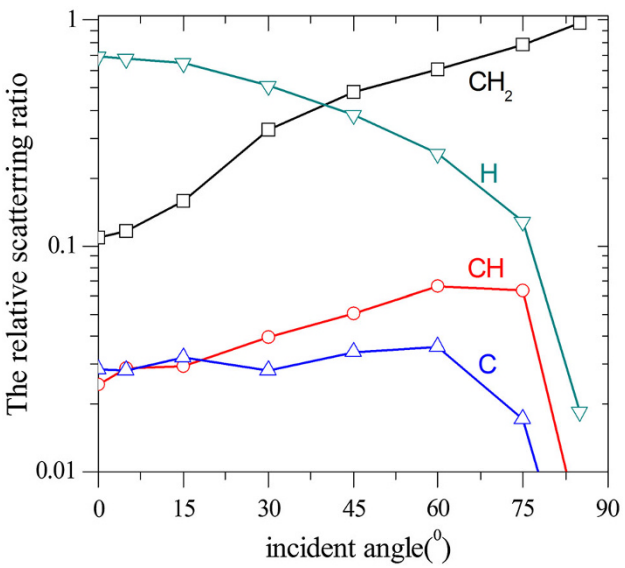

Fig. 5 The scattering ratio of the number of scattered particles to the total number of scattered particles

4 Conclusions

Our simulations show that the deposition ratio of C and H atoms has a strong dependence on the incident angle. When the incident angle exceeds a threshold value the composite particle CH_2 is mainly reflected. The carbon atoms are much more easily bonded to the tungsten atoms than hydrogen atoms, though a few of the latter can also penetrate into the tungsten sample. When the incidence angle is greater than 75°, the kinetic energy of the particles exceeds significantly the bound energy. Below this angle, an effective W–C bonding occurs, which results in a W–C layer of about 0.5 nm with another C, H-rich layer depositing on top of it. It is clear that our studies on the interactions between the plasma and the first-wall materials are still not complete. Some interesting issues such as the consequences of choosing different hydrocarbon groups, the different crystal plane of $\alpha - W$, e.g., (011), (111), etc., the different incident energy of the particulates, etc., are also very important in understanding the interactions between the plasma and the first-wall materials. It is thus worthy of further studies to clarify these issues.

It should be pointed that our preliminary study has mainly involved the interactions between the possible particles produced in the fusion chamber and the first-wall materials, i.e., tungsten steel. The role of carbon and the other elements in enhancing and improving the properties of a specific material has not been studied, though it is very important, otherwise we even do not have the concept of steel. The point raised here is that chemical composition does not uniquely decide the properties of a steel, in almost

all cases, the treatment processes such as heat treatment processes are also very crucial. This implies that the microstructure of a material is the dominating factor.

For example, the microstructure of rail steel is composed of pearlite, while that of low carbon steel used for railway sleepers consists of ferrite and cementite [19]. The properties, such as the hardness, wear resistance, tensile strength, etc., depend actually on the multi-scale structures, say, the composition, the proportion of different structural domains and the details of each domain. The MD simulation, a powerful tool to study the structure at the atomic length scale, has proved to be an efficient approach, as we have shown in this work, to reveal the relations between the microstructures of various complicated steels and their properties. Our future work will be done along this line for both fusion reactor materials and railway track materials.

Acknowledgments This work is financially supported by the Science Foundation for International Cooperation of Sichuan Province (2014HH0016), the Fundamental Research Funds for the Central Universities (SWJTU2014: A0920502051113-10000), National Magnetic Confinement Fusion Science Program (2011GB112001).

References

1. Bolt H, Barabash V, Krauss W et al (2004) Materials for the plasma-facing components of fusion reactors. J Nucl Mater 329–333:66–73
2. Loarte A, Lipschultz B, Kukushkin AS et al (2007) Chapter 4: power and particle control. Nucl Fus 47(6):203–263
3. YueLin Liu, HongBo Zhou, Ying Zhang et al (2011) Interaction of C with vacancy in W: a first-principles study. Comput Mater Sci 50(11):3213–3217
4. Zhongshi Yang, Xu Q, Junqi Liao et al (2009) Study on C-W interactions by molecular dynamics simulations. Nucl Instrum Methods Phys Res Sect B 267(18):3144–3147
5. Miyahara A, Tanabe T (1988) Graphite as plasma facing material. J Nucl Mater 155–157:49–57
6. Grote H, Bohmeyer W, Kornejew P et al (1999) Chemical sputtering yields of carbon based materials at high ion flux densities. J Nucl Mater 266–269:1059–1064
7. Janev Ratko K, Reiter Detlev (2002) Collision processes of hydrocarbon species in hydrogen plasmas: I. the methane family. Berichte des Forschungszentrums Jülich, Zentralbibliothek. ISBN 0944-2952
8. Winter J (1998) Dust in fusion devices—experimental evidence, possible sources and consequences. Plasma Phys Controll Fus 40(6):1201
9. Winter J, Gebauer G (1999) Dust in magnetic confinement fusion devices and its impact on plasma operation. J Nucl Mater 266–269:228–233
10. Winter J (2000) Dust: a new challenge in nuclear fusion research? Phys Plasmas 7(10):3862
11. Sugai H, Mitsuoka Y, Toyoda H (1998) Observation of surface dissociation of low-energy polyatomic ions relevant to plasma processing. J Vac Sci Technol A 16(1):290–293
12. Fukumoto M, Kashiwagi H, Ohtsuka Y et al (2009) Hydrogen behavior in damaged tungsten by high-energy ion irradiation. J Nucl Mater 386–388:768–771
13. Ohya K, Inai K, Kikuhara Y et al (2011) Molecular dynamics study on hydrocarbon interaction with plasma facing walls. J Nucl Mater 417(1–3):637–642
14. Ohya K, Kikuhara Y, Inai K et al (2009) Simulation of hydrocarbon reflection from carbon and tungsten surfaces and its impact on co-deposition patterns on plasma facing components. J Nucl Mater 390–391:72–75
15. Swope WC, Andersen HC, Berens PH, Wilson KR (1982) A computer simulation method for the calculation of equilibrium constants for the formation of physical clusters of molecules: application to small water clusters. J Chem Phys 76(1):637
16. Juslin N, Erhart P, Träskelin P et al (2005) Analytical interatomic potential for modeling nonequilibrium processes in the W–C–H system. J Appl Phys 98(12):123520
17. Kensuke Inai, Kikuhara Y, Kaoru Ohya (2008) Comparison of carbon deposition on tungsten between molecular dynamics and dynamic Monte Carlo simulation. Surf Coat Technol 202(22–23):5374–5378
18. Berendsen HJC, Postma JPM, van Gunsteren WF et al (1984) Molecular dynamics with coupling to an external bath. J Chem Phys 81(8):3684
19. Resources and news for science education: http://resources.schoolscience.co.uk/Corus/16plus/steelch3pg4.html. Accessed 9 Aug 2003